Placement of a Fast Ion Loss Detector Array in Wendelstein 7-X

D. Kulla[1], S. Lazerson[1], S. Günter[2], M. Hirsch[1], D. Hartmann[1],
P. McNeely[1], N. Rust[1], R. C. Wolf[1], and the W7-X Team
[1] *Max-Planck Institut für Plasmaphysik, Greifswald, Germany*
[2] *Max-Planck Institut für Plasmaphysik, Garching, Germany*

Good confinement of α particles (He4-ions) is an essential requirement for a Stellarator fusion reactor. In contrast to Tokamak reactors with largely axisymmetric configuration, such confinement is not easy to achieve in Stellarators. To alleviate this issue, Wendelstein 7-X (W7-X) was optimized in this regard. As the experimental confirmation of the success of this optimization is pending, a novel in-wall tile fast ion loss detector is currently being developed to aid in this assessment [1]. the detector has a compact form factor, giving large flexibility in its mounting position. Furthermore, it allows installation of an array of detectors, which is beneficial as hot spots of fast ion losses change their position and magnitude depending on the configuration, as can be seen in figure 1. No estimate of global losses can therefore be made from a single measurement position, and a detector array is needed.

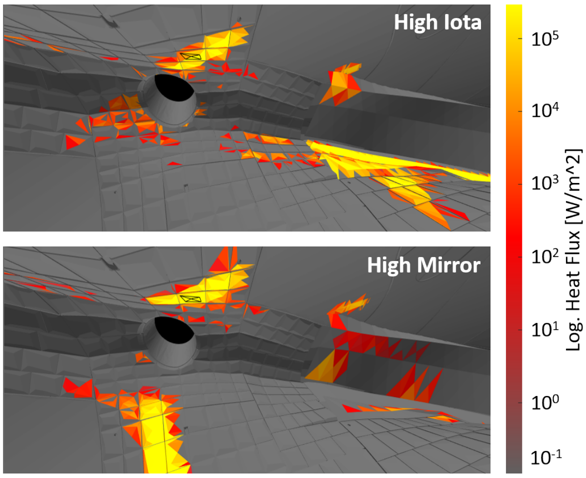

Figure 1: Comparision of the heat flux generated by lost fast ions for high mirror and high iota magnetic configurations with otherwise equal parameters.

Here, we present results from simulations of neutral beam injected (NBI) fast ion orbits, which inform the placement of these detectors. BEAMS3D was used to simulate neutral beam deposition and subsequent slowing down of the fast particle markers up to the last closed flux surface (LCFS) in gyro-center approximation. This code has recently been validated for its deposition model [2] and its capabilities simulating the slowing down have been investigated [3]. ASCOT5 was then used to simulate the markers in full orbit up to the wall [4]. Increasing marker numbers between the two simulations improves statistics on the wall tiles while keeping computational load under control. The simulation yields estimates of the particle distributions at the wall, which can be used to determine positions of high fast ion losses for various plasma configurations.

In the investigation presented here, we consider two sets of simulations: a scan in plasma β in the high mirror configuration (1) and a configuration scan, consisting of standard, high

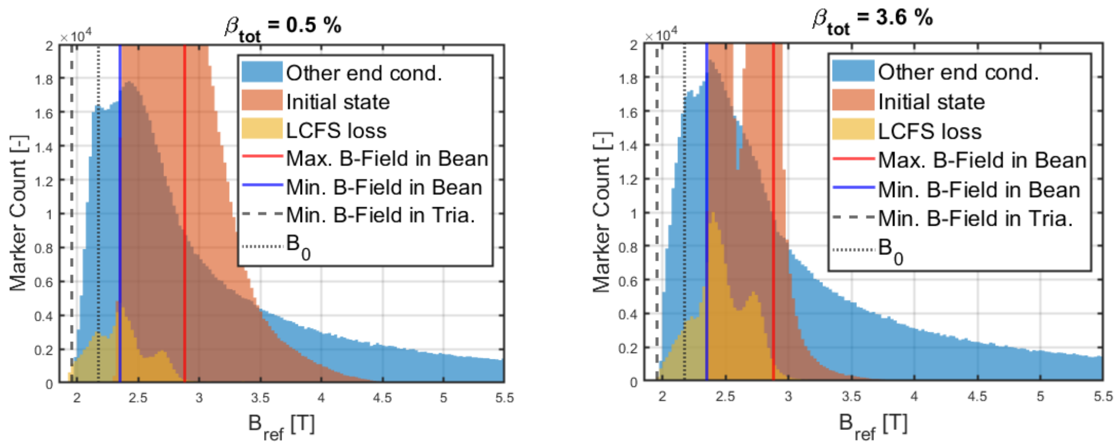

Figure 2: Spectra in B_{ref} of the initial injected fast ion population (high mirror configuration), as well as the thermalized and escaping populations at the last closed flux surface. The initial state shows that the NBI injects hardly any deeply trapped particles for either case.

mirror and high iota magnetic configurations (2). Each simulation was based on vacuum and equlibrium magnetic fields as well as neoclassical transport simulations for realistic profiles. Evaluation of the global losses in each simulation revealed an increase of lost particles with plasma β. For the high β case, the magnetic field becomes quasi-isodynamic, i.e. the radial guiding-center drift velocity of toroidally trapped particles should average to zero as the poloidal drift direction is unhindered. The property holds only for collisionless orbits however, and it requires high plasma pressure, i.e. high values of β.

To identify collisionless particle orbits, consider the following for the reflection point of a particle, where its velocity parallel to the magnetic field changes sign. The magnetic field at this point is denoted B_{ref}, and for the local magnetic field at the particle position B where $v = v_\perp$:

$$B_{\text{ref}} = B\frac{1/2mv^2}{1/2mv_\perp^2} = \frac{E_{\text{kin,ref}}}{\mu} = B\frac{v^2}{v_\perp^2}. \tag{1}$$

Where m is the particle mass, $v_\perp$ its velocity perpendicular to the magnetic field, and $E_{\text{kin,ref}}$ the kinetic energy. The subscript indicates that in the reflection point, all kinetic energy is perpendicular to the field. As both the kinetic energy and magnetic moment are conserved quantities in an adiabatic field, collisionless particle orbits can be classified according to B_{ref} [5].

In figure 2, the deeply trapped, trapped-passing boundary and passing particles are distinguished by the minimum and maximum magnetic field of the bean-shaped cross-section. Along the filed lines, the maximum field strengths occur there, so it acts as the barrier between Stellarator symmetric sections (field period). If a particle has a B_{ref} value lower than the minimum field of the bean, it is trapped in a single field period and thus considered deeply trapped here.

The figure shows that barely any such particle orbits are present in the initial state after being injected by the NBI system. However these orbits are populated by slowing down and pitch-angle scattering processes in the collisional plasma. From the two spectra shown in figure 2 it is clear that the particle losses increase with plasma β, but mainly do so in the trapped-passing region. This increase is not caused by an increase in NBI deposition: Comparing the ratios of ionized particle flux (fast particles generated by the NBI) to that of particles exiting the LCFS we see an increase from 7.4% (low β) to 12.9% (high β). This fraction should stay constant if the rise was caused by the increased deposition at high densities.

Even though the quasi-isodynamic behaviour most likely will not be observable with NBI particles, the experimental experience from previous operations still makes the construction of a detector array for it worthwhile. The array shown in figure 3 consists of 16 detectors in total, including three toroidal arrays with five detectors each. From the simulation data, the reproduction of the global losses by the array can be determined. The marker weight (particle flux) is investigated here, as the detectors will measure current, which is proportional to particle flux.

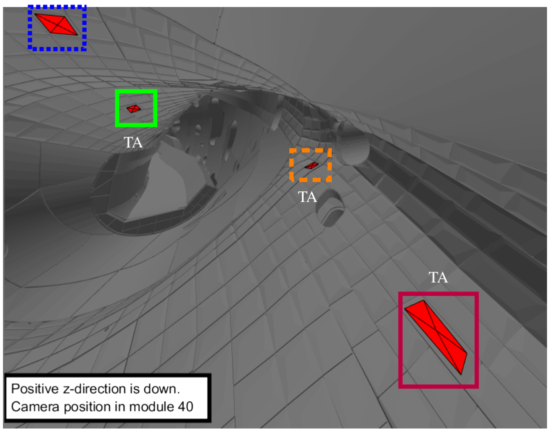

Figure 3: View of the detector positions. TA indicates a toroidal array.

Figure 4 shows that the array qualitatively reproduces the losses for all plasma configurations under consideration here except the $\beta = 0.5\%$ case. It has a higher amplitude in the detected weight than the $\beta = 2.0\%$ case, while the total weight is a little lower for the lower β configuration. When excluding the green marked positions, the losses are qualitatively reproduced for the three cases. Over all runs, the detected weight is roughly 0.5% of the global weight. It corresponds to all markers in the selected areas shown in 3. The actual measurements will thus have a much lower fraction due to the detector aperture and geometry not considered here.

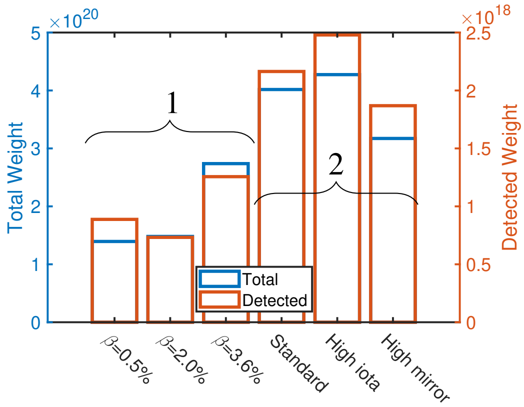

Figure 4: Comparison of detected to global lost marker weight (particles/s). Note the different scales for the vertical axes.

The configuration dependence of losses observed in figure 1 is also clearly visible in figure

5, as every detector position has a distinct response in the different simulations. In the orange marked array, the differences between toroidal positions are most pronounced, which is due to the wall geometry changing substantially. The similarity in the red and green arrays indicates that a reduction of positions could be possible, depending on installation complexity and cost. The current predicted by the simulation is on the order of 10 mA, which is well measurable. However, closer analysis is necessary as effects such as charge exchange processes are not taken into account here.

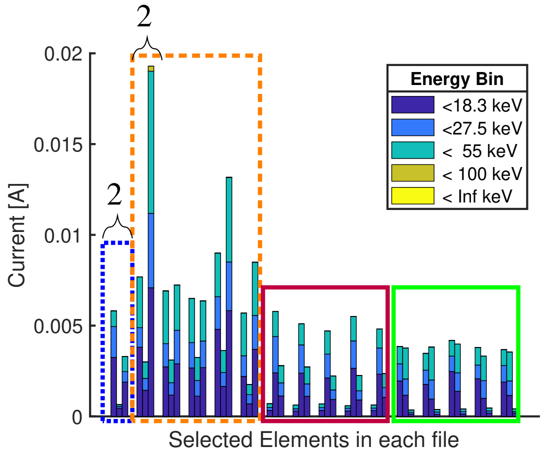

Figure 5: Current distribution for the energy bins and detector positions in the array, for the 2nd set of simulations as shown in 4.

This detector array is thus expected to yield appreciable measurements for the studied cases. For other plasma configurations, more simulations similar to the ones carried out here need to be conducted to determine its behaviour. There is currently no trivial way to predict the real and phase space distribution of fast ion losses, so forward modelling is necessary. Considering the detectors, the complex nature of the fast ion loss pattern requires measurement of the losses at multiple locations, and complementing these by resolved measurements of the velocity space distribution. Investigation of the quasi-isodynamic particle behavior is hindered by the fact that the NBI hardly generates deeply trapped particles. This is caused by the proximity of the NBI system to the bean shaped cross section, and subsequent high magnetic fields, causing in turn high reflection magnetic fields of the generated particles. The implementation of a neutral beam closer to the triangular cross section, where the magnetic field is lower, seems necessary to access the quasi-isodynamic regime. Initial assessment of this geometry appears promising but detailed analysis is left to future work. This beam should also have a higher injection energy than the current 55 keV generated by the NBI to generate collisionless particles.

References

[1] S. Lazerson *et al.*, Rev. Sci. Instruments **90**, 9 (2019)

[2] M. McMillan and S. Lazerson, Plasma Phys. Control. Fusion **56**, 9 (2014)

[3] S.A. Lazerson *et al.*, submitted to Nucl. Fusion (2021)

[4] J. A. Heikkinen and S.K. Sipila, Phys. Plasmas **2**, 10 (1995)

[5] J. M. Faustin *et al.*, Nucl. Fusion **56**, 9 (2016)